
Characterization of ^{18}F -FPyKYNE-Losartan for Imaging AT_1 Receptors

Maryam Hachem^{1,2}, Mario Tiberi^{2,3}, Basma Ismail^{1,2}, Chad R. Hunter¹, Natasha Arksey^{1,2}, Tayebah Hadizad¹, Rob S. Beanlands^{1,2}, Robert A. deKemp¹, and Jean N. DaSilva^{1,2,4}

¹National Cardiac PET Centre, University of Ottawa Heart Institute, Ottawa, Ontario, Canada; ²Department of Cellular and Molecular Medicine, University of Ottawa, Ottawa, Ontario, Canada; ³Ottawa Hospital Research Institute (Neuroscience Program), Ottawa, Ontario, Canada; and ⁴Department of Radiology, Radio-Oncology and Nuclear Medicine, University of Montreal, University of Montreal Hospital Research Centre (CRCHUM), Montréal, Québec, Canada

Most physiologic effects of the renin angiotensin system (RAS) are mediated via the angiotensin (Ang) type 1 receptor (AT_1R). The ^{18}F -FPyKYNE derivative of the clinically used AT_1R blocker losartan exhibits high binding selectivity for kidney AT_1R and rapid metabolism in rats. The aim of this study was to further assess the binding profile of this novel PET agent for imaging AT_1R in rats and pigs. **Methods:** In vitro binding assays were performed with ^{18}F -FPyKYNE-losartan in rat kidneys. Male Sprague-Dawley rats were used to assess dosimetry, antagonistic efficacy via blood pressure measurements, and presence of labeled metabolites in kidneys. Test-retest PET imaging, blocking with AT_1R antagonist candesartan (10 mg/kg), and plasma metabolism analysis were performed in female Yorkshire pigs. **Results:** ^{18}F -FPyKYNE-losartan bound with high affinity (dissociation constant of 49.4 ± 18.0 nM and maximal binding of 348 ± 112 fmol/mm²) to rat kidney AT_1R . It bound strongly to plasma proteins in rats (97%), and its labeled metabolites displayed minimal interference on renal AT_1R binding. FPyKYNE-losartan fully antagonized the Ang II pressor effect, albeit with 4-fold potency reduction (the effective dose inhibiting 50% of the Ang II-induced maximal pressor response of 25.5 mg/kg) relative to losartan. PET imaging exhibited high kidney-to-blood contrast and slow renal clearance, with an SUV of 14.1 ± 6.2 . Excellent reproducibility was observed in the calculated test-retest variability ($7.2\% \pm 0.75\%$). Only hydrophilic-labeled metabolites were present in plasma samples, and renal retention was reduced (~60%) at 10–15 min after blockade with candesartan. **Conclusion:** ^{18}F -FPyKYNE-losartan has a favorable binding profile and displays high potential for translational work in humans as an AT_1R PET imaging agent.

Key Words: RAS; AT_1R specific binding; metabolism; dosimetry; PET imaging studies in rats and pigs

J Nucl Med 2016; 57:1612–1617
DOI: 10.2967/jnumed.115.170951

Hyperactivity of the renin angiotensin system (RAS), and specifically the pathologic alteration in angiotensin II (Ang II)

Received Dec. 7, 2015; revision accepted Apr. 11, 2016.

For correspondence or reprints contact: Jean N. DaSilva, Department of Radiology, Radio-Oncology and Nuclear Medicine, University of Montreal, University of Montreal Hospital Research Centre (CRCHUM), 900 Rue Saint-Denis, Montréal, Québec, H2X 0A9 Canada.

E-mail: jean.dasilva@umontreal.ca

Published online May 19, 2016.

COPYRIGHT © 2016 by the Society of Nuclear Medicine and Molecular Imaging, Inc.

type 1 receptor (AT_1R), is thought to play a distinct role in the development of disease processes including hypertension, myocardial infarction, chronic kidney disease, and cardiorenal failure (1–3). Conflicting results have been reported on AT_1R levels measured under pathophysiologic conditions. Although previous PET studies have been performed with small (rodents) and larger (dogs, baboons, pigs) animals (4–6) using ^{11}C -labeled AT_1R ligands, no research has been published using an ^{18}F -labeled AT_1R ligand. ^{18}F -labeled tracers offer some key advantages over ^{11}C , including a longer half-life (109.6 vs. 20.4 min) (7), enabling multiple scans from a single formulation and shipment to other sites and higher image resolution due to lower energy and shorter positron range (0.23 vs. 0.39 mm in soft tissue) (8), thus enabling higher image resolution.

Previous structure-activity relationship studies demonstrated that large prosthetic groups can be introduced at the imidazole 5-position of losartan with minimal changes in binding properties (9). Moreover, addition of a leucine and a short linker composed of tetraethylene glycol and diglycolic acid between the losartan moiety and the tetra-amine chelator yielded to a losartan analog displaying high affinity (inhibitory constant = 6 nmol/L) for AT_1R (10). Recently, ^{18}F -FPyKYNE-losartan was synthesized by conjugation of ^{18}F -FPyKYNE with the azide-modified trityl losartan via click chemistry with high chemical and radiochemical purities (11). Preliminary in vivo evaluation of ^{18}F -FPyKYNE-losartan with PET imaging displayed a dose-dependent reduction of this radiotracer in rat kidney AT_1R s and binding selectivity for AT_1R over AT_2R . Additionally, ^{18}F -FPyKYNE-losartan is metabolized into mostly hydrophilic-labeled products in rat plasma, suggesting minimal interference of the ^{18}F -labeled metabolites with AT_1R binding (11).

The specific aims of the present study were to evaluate the binding affinity of ^{18}F -FPyKYNE-losartan to renal AT_1R s and antagonistic efficacy on Ang II pressor effect in rats; the relative proportions of labeled metabolites (if any) in rat kidney and pig plasma, compared with unchanged tracer using column-switch high-performance liquid chromatography (HPLC); the biodistribution and radiation dosimetry; and the PET imaging profile of ^{18}F -FPyKYNE-losartan in pigs.

MATERIALS AND METHODS

Animals

All animal experiments were conducted in accordance with the Canadian Council on Animal Care guidelines and approved by the Animal Care Committee of the University of Ottawa. Male and female (for dosimetry) Sprague-Dawley rats (200–300 g) (Charles River) were housed in pairs and maintained on a 12-h light-dark cycle with

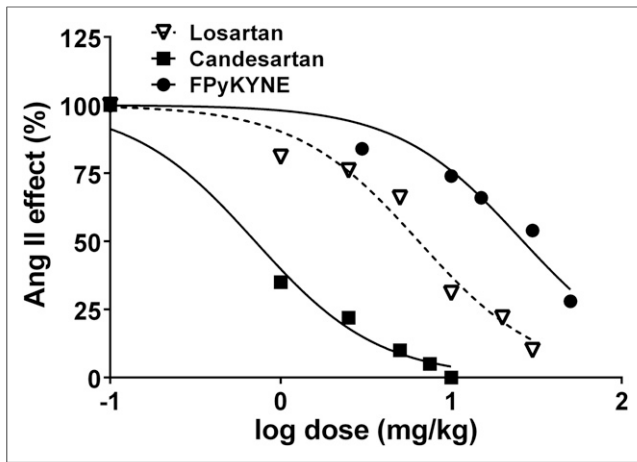


FIGURE 2. Dose–response curves of AT₁R blockers candesartan, losartan, and FPYKYNE-losartan displaying their effect in blocking Ang II pressor response (submaximal dose, 3 μg/kg intravenously) in anesthetized rats. Curves were analyzed with nonlinear curve-fitting program (GraphPad Prism 6.02) using 4-parameter logistic equation. Curves were fitted with shared Hill slope factor.

were coregistered with their corresponding PET scans, to ensure accurate localization of regions of interest. Arterial time–activity curves were corrected for partial-volume losses based on a computer simulation of the PET image resolution and the aorta radial dimension measured on the CT angiography images. ¹⁸F-FPYKYNE-losartan renal activity was measured as SUV (g/mL) at 10–15 min after injection (frame 20) (22). The specific binding index was expressed as the reduced peak retention in the renal cortex and was calculated from the difference in peak SUVs between baseline and blocking conditions.

Radiolabeled Metabolite Analysis in Plasma. During the PET scans, blood samples were collected from the femoral artery at –5 (control), 1, 2, 5, 10, 20, and 40 min after injection (*n* = 3). Plasma samples were prepared as described previously (11,19). Control plasma was spiked with 0.37 MBq of tracer, filtered, and then injected onto the HPLC system.

Arterial Input Function Corrections. The first step toward generating an arterial input function was correcting for plasma radioactivity. To correct for binding to red blood cells, activity in whole blood and in plasma was measured at serial time points, and the plasma–to–whole-blood ratio was determined as a function of time. ¹⁸F-FPYKYNE-losartan (5 MBq/kg) was injected via the ear vein and arterial blood (5–6 mL) collected from the femoral artery at 0.5, 1, 2, 5, 10, 20, 40, 60, and 90 min. Blood samples were weighed and counted for activity. Samples were centrifuged to obtain plasma and then weighed and counted to determine activity per gram (19).

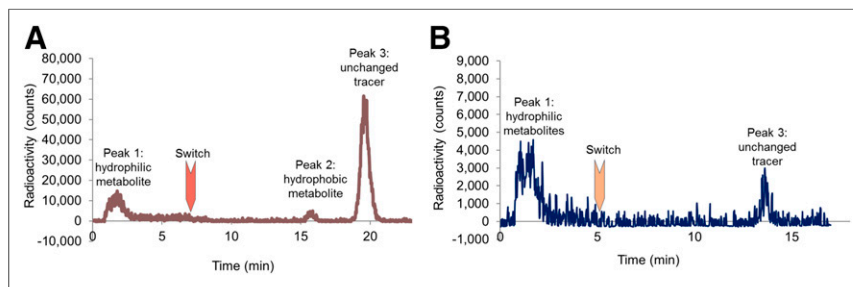


FIGURE 3. Representative high-performance liquid chromatograms displaying unchanged ¹⁸F-FPYKYNE-losartan (peak 3) and its labeled hydrophilic (peak 1) and hydrophobic (peak 2) metabolites in rat kidney (A) and pig plasma (B) at 10-min time point.

Statistical Analysis

All results are expressed as mean ± SD or ± SE as indicated. Means were compared using the *t* test (paired or unpaired). The test–retest variability was calculated by taking the ratio of the absolute value of the difference between repeated measurements and the mean of the repeated measurements as described by Lortie et al. (19).

RESULTS

In Vitro Binding in Rat Kidneys

¹⁸F-FPYKYNE-losartan binding displayed a discrete localization in the kidney. The highest level of total binding relative to NSB was detected in the kidney cortex. Global curve-fitting analyses of paired total binding and NSB curves revealed that ¹⁸F-FPYKYNE-losartan bound to kidney cortex with a *K_D* of 49.4 ± 18.0 nM and maximal binding of 348 ± 112 fmol/mm².

In Vivo Antagonism in Rats

Ang II caused a dose-dependent increase in blood pressure, and the submaximal dose was determined graphically to be 3 μg/kg. Losartan and candesartan exhibited a dose-dependent antagonism of AT₁Rs and virtually abolished the Ang II effect at doses of 30 and 10 mg/kg, respectively. The blocking effect of FPYKYNE-losartan obtained at a dose of 50 mg/kg was 72%. The computed effective doses inhibiting 50% of the Ang II–induced maximal pressor response values (in mg/kg) obtained with the curve-fitting analysis of inhibitory dose–response curves were 0.7 (candesartan), 6.4 (losartan), and 25.5 (FPYKYNE-losartan) (Fig. 2). FPYKYNE-losartan also displayed full antagonism but with less potency than losartan and candesartan.

Radiolabeled Metabolite Analysis in Rat Kidneys

¹⁸F-FPYKYNE-losartan was bound at 97% to plasma proteins. As described in rat plasma (11), kidney samples revealed 3 major HPLC peaks (Fig. 3A). The hydrophilic-labeled metabolite (peak 1) increased slowly over time, whereas the hydrophobic metabolite (peak 2) had a negligible contribution to the total activity. Unchanged ¹⁸F-FPYKYNE-losartan (peak 3) accounted for more than 50% of total radioactivity at all time points (Table 1). Blockade of AT₁Rs with candesartan produced a reduction in unchanged tracer proportion by 74% and 88% with the 5 and 10 mg/kg doses, respectively. The proportion of hydrophobic metabolite decreased by half at a blocking dose of 10 mg/kg, whereas hydrophilic metabolite proportion increased by 86% at the same blocking dose (Table 1).

Rat Dosimetry Studies

The decay-corrected accumulation of radioactivity in whole tissues is depicted in Supplemental Table 1. Most tissues demonstrated a rapid tracer uptake, with levels gradually decreasing after 5 min. Similar trends were observed for both men and women. Elevated radioactivity accumulation with time occurred within the metabolism-related tissues (liver, small intestine contents, upper and lower intestine contents, and urine). The liver showed the highest uptake and accounted for around 30% of the effective dose (ED) in both sexes (Supplemental Table 2). The sex-averaged ED calculated using both ICRP 60 and 103 was 0.031 mSv/MBq. A mean of 85% of the total injected dose was recovered in the organs and carcass at the time points studied.

TABLE 1
Proportions of Unchanged ^{18}F -FPyKYNE-Losartan and Its Labeled Metabolites in Rat Kidney Homogenate at Respective Time Points

Peak	Identity	0 min	5 min	10 min*			20 min	30 min
				0 mg/kg	5 mg/kg	10 mg/kg		
1	Hydrophilic metabolite	0 ± 0	5 ± 4	12 ± 1	76 ± 20	88 ± 15 ^{†‡}	17 ± 8	39 ± 20
2	Hydrophobic metabolite	0 ± 0	2 ± 1	4 ± 2	2 ± 2 [†]	2 ± 0 [†]	5 ± 2	3 ± 2
3	Unchanged tracer	100 ± 0	93 ± 4	84 ± 2	22 ± 20 [†]	10 ± 14 [†]	78 ± 10	58 ± 19

*Data are given for 3 different candesartan blocking doses.

[†] $P < 0.05$, compared with baseline.

[‡]Compared with previous dose.

PET Imaging of Pig Kidneys

Time–activity curves derived from the right kidney exhibited high kidney-to-blood contrast (ratio of approximately 3) and slow clearance from the kidneys (Fig. 4A). The highest renal uptake was obtained at 10–15 min after injection, with an SUV of 14.1 ± 6.15 . Test and retest scans were reproducible with a test–retest variability of $7.2\% \pm 0.75\%$ and a P value of 0.89, showing no significant difference between the datasets. Blocking AT_1Rs with 10 mg/kg of candesartan resulted in reduced renal ^{18}F -FPyKYNE-losartan retention (Fig. 4B). SUV_{max} (at 10–15 min) in the right kidney was significantly decreased from 14.1 ± 6.15 to 5.8 ± 4.60 ($P = 0.03$). This 60% reduction demonstrates specific binding of ^{18}F -FPyKYNE-losartan to AT_1Rs in pig kidneys. The arterial plasma-to-whole-blood ratio (1.4) was almost constant over time (0–90 min), facilitating input function correction. However, further corrections are necessary for accurate quantification, including correction for labeled metabolites and plasma-protein binding.

Radiolabeled Metabolite Analysis in Pig Plasma

Only peak 1 (hydrophilic metabolite) and peak 3 (unchanged tracer) were present in pig plasma in both normal and blocking conditions (Fig. 3B). At 20 min, less than 10% of radioactivity (noise- and decay-corrected) in normal plasma was associated with unchanged tracer (Table 2). Blocking AT_1Rs resulted in a faster metabolism in pig plasma at 20 min (Table 2). A significant difference in the proportion of unchanged ^{18}F -FPyKYNE-losartan between normal and blocking conditions was identified at 5, 10, and 20 min ($P = 0.008, 0.02, \text{ and } 0.04$, respectively).

DISCUSSION

Successful development of a new noninvasive ^{18}F -labeled molecular imaging probe for quantifying AT_1Rs would present a

unique opportunity to advance understanding and contribution of AT_1Rs to the progression of cardiovascular and renal diseases and a means to directly measure therapy responses to optimize patient outcomes. ^{18}F -FPyKYNE-losartan small-animal PET images obtained previously (11) displayed high tissue contrast in the kidney cortex and outer medulla, which correlates well with the known physiologic distribution of AT_1R (24). Nonetheless, the cortical and medullary binding could not be differentiated, which can be attributed to the image resolution of the small-animal PET. In the current study, FPyKYNE-losartan exhibited high in vitro binding affinity to AT_1R in the renal cortex and full in vivo antagonism, similar to its parent compound losartan. However, a higher dosage of FPyKYNE-losartan was required for blocking Ang II pressor response relative to losartan and candesartan (4 and 36 times more potent, respectively). The order of potency of candesartan and losartan in vivo is consistent with the in vitro binding affinities of these AT_1R blockers reported previously (13,25).

Binding of a drug to plasma and tissue proteins inhibits drug disposition and has important effects on drug dynamics because only the free (unbound) drug interacts with receptors. ^{18}F -FPyKYNE-losartan exhibits similar plasma-protein binding to its parent compound losartan (97% and 98%, respectively). Thus, only 3% of ^{18}F -FPyKYNE-losartan is freely available for binding to tissue AT_1R . ^{18}F -FPyKYNE-losartan kidney metabolite analysis displayed slow accumulation of the hydrophilic-labeled metabolite and the presence of almost 60% unchanged tracer at 30 min after injection. Blocking AT_1R with candesartan, whereas a significant increase was observed in the proportion of the hydrophilic metabolite. These results indicate that the portion of the signal corresponding to AT_1R -specific binding is mostly from the unchanged tracer because of the proportion of the labeled metabolites that is not reduced after AT_1R blockade in rat kidneys.

Rat dosimetry data suggest that the hepatobiliary system is primarily responsible for eliminating ^{18}F -FPyKYNE-losartan from the body, whereas the kidneys are the secondary route of excretion. Losartan is known to be primarily eliminated via the cytochromes-P450 system in the liver (26,27). As a major site for drug metabolism, the liver aids in the elimination

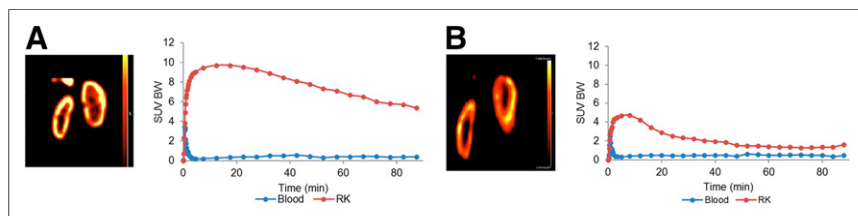


FIGURE 4. Representative PET image (coronal view) of pig kidneys displaying ^{18}F -FPyKYNE-losartan uptake in normal (A) and blocking (B) conditions. Tracer time–activity curves for blood input (aorta) and right kidney (RK) are presented as SUVs normalized to body weight (SUV_{BW}) from 0 to 90 min.

TABLE 2
Proportions of ¹⁸F-FPyKYNE-Losartan and Its Hydrophilic-Labeled Metabolites in Pig Plasma in Normal and Blocking Conditions

Condition	Identity	Time point (min)						
		0	1	2	5	10	20	40
Baseline	Hydrophilic metabolite (%)	0 ± 0	0 ± 0	0 ± 0	32 ± 6	83 ± 2	94 ± 4	100 ± 0
	Unchanged tracer (%)	100 ± 0	100 ± 0	100 ± 0	68 ± 6	17 ± 2	6 ± 4	0 ± 0
Blocking	Hydrophilic metabolite (%)	0 ± 0	0 ± 0	3 ± 13	68 ± 21	96 ± 0	99 ± 3	100 ± 0
	Unchanged tracer (%)	100 ± 0	100 ± 0	97 ± 12	32 ± 15*	4 ± 1*	1 ± 2*	0 ± 0

**P* < 0.05 compared with baseline.

n = 3 per time point.

process by converting lipid-soluble substances into more hydrophilic compounds to be easily excreted by the kidneys (28). Hence, for hydrophobic compounds such as FPyKYNE-losartan, the hepatobiliary pathway is the main elimination route. The sex-averaged ED value calculated using ICRP 60 and 103 (0.031 mSv/MBq) is comparable to other ¹⁸F tracers such as 2-¹⁸F-fluoro-A-85380 (ED = 0.028 mSv/MBq), *O*-(2-¹⁸F-fluoroethyl)-L-tyrosine (ED = 0.016 mSv/MBq), and ¹⁸F-FDG (ED = 0.024 mSv/MBq) (29–31). EDs calculated for ¹⁸F-FPyKYNE-losartan are well below the regulatory limits recommended by the Food and Drug Administration (28). Although the RAS is known to differ between rats, pigs, and humans, the dose-limiting organs associated with common hepatobiliary metabolism and clearance pathways are likely to remain similar between species. Therefore, the dosimetry profile of ¹⁸F-FPyKYNE-losartan is within safe limits for approval of use in human studies.

PET imaging studies in pigs revealed higher image contrast and slower clearance of the tracer from the kidneys than in rats. The long residence time at the receptor and high tissue retention are expected with the long dissociation time of losartan in humans (67 min) (25,32,33). Reproducible results and imaging procedure provide evidence that the quantification of tracer uptake using SUVs is reliable in large animals. For accurate quantification, further arterial input corrections are required, namely metabolite correction for authentic parent tracer in plasma from arterial blood. Blockade of AT₁Rs with candesartan reduced peak retention (~ 60%) at 10–15 min in the renal cortex, further confirming binding specificity of ¹⁸F-FPyKYNE-losartan to AT₁Rs. Thereby, the PET signal in pigs is expected to represent unchanged ¹⁸F-FPyKYNE-losartan and NSB. Normal pig plasma exhibited faster ¹⁸F-FPyKYNE-losartan metabolism than rat plasma, because complete clearance from pig plasma was detected at 30 min whereas 23% of unmetabolized tracer was still present in rat plasma at that time (13). When AT₁Rs were blocked with candesartan, this process was even faster, with only 4% of the total radioactivity from unchanged tracer at 10 min and complete clearance of ¹⁸F-FPyKYNE-losartan from plasma at 20 min. The presence of hydrophilic metabolites only, not binding to AT₁Rs, should facilitate accurate blood input function corrections and kinetic modeling calculations for quantification of AT₁Rs in future studies. Confirmation of similar binding characteristics and high signal-to-noise ratio of the ¹⁸F-FPyKYNE structural analog of the clinically used losartan will facilitate translational work to humans.

CONCLUSION

¹⁸F-FPyKYNE-losartan binds with high affinity to renal AT₁Rs, and this novel radioligand displays full antagonism for Ang II pressor effect. The metabolism studies in small and large animals revealed that the labeled metabolites do not bind to renal AT₁Rs facilitating quantitative PET imaging. The sex-averaged ED of ¹⁸F-FPyKYNE-losartan is within an acceptable range compared with other ¹⁸F-labeled tracers. Reproducible PET images obtained in pigs combined with favorable binding profile support the potential of ¹⁸F-FPyKYNE-losartan for translational work in humans as an AT₁R PET imaging agent.

DISCLOSURE

The costs of publication of this article were defrayed in part by the payment of page charges. Therefore, and solely to indicate this fact, this article is hereby marked “advertisement” in accordance with 18 USC section 1734. This work was supported in part by grants from the Canadian Institutes of Health Research (MOP-126079 to JD and MOP-125878 to MT), Ontario Preclinical Imaging Consortium (MRI ORF #RE03-51). Rob S. Beanlands is a career investigator supported by the Heart and Stroke Foundation of Ontario, a Tier 1 University of Ottawa chair in Cardiovascular Imaging Research, and the Ottawa Heart Institute’s Vered chair. No other potential conflict of interest relevant to this article was reported.

ACKNOWLEDGMENTS

We thank the radiochemistry staff (Yanick Lee), Richard Seymour, Julia Petryk, and Marika Kolajova for assistance.

REFERENCES

- de Gasparo M, Catt KJ, Inagami T, Wright JW, Unger T. International union of pharmacology. XXIII: the angiotensin II receptors. *Pharmacol Rev*. 2000;52: 415–472.
- Billet S, Aguilar F, Baudry C, Clauser E. Role of angiotensin II AT₁ receptor activation in cardiovascular diseases. *Kidney Int*. 2008;74:1379–1384.
- Wassmann S, Nickenig G. Pathophysiological regulation of the AT₁-receptor and implications for vascular disease. *J Hypertens Suppl*. 2006;24(suppl 1): S15–S21.
- Owonikoko TK, Fabucci ME, Brown PR, et al. In vivo investigation of estrogen regulation of adrenal and renal angiotensin (AT₁) receptor expression by PET. *J Nucl Med*. 2004;45:94–100.
- Szabo Z, Kao PF, Burns HD, et al. Investigation of angiotensin II/AT₁ receptors with carbon-11-L-159,884: a selective AT₁ antagonist. *J Nucl Med*. 1998;39: 1209–1213.

6. Szabo Z, Speth R, Brown P, et al. Use of positron emission tomography to study AT₁ receptor regulation in vivo. *J Am Soc Nephrol*. 2001;12:1350–1358.
7. Gad SC, ed. *Pharmaceutical Manufacturing Handbook: Production and Processes*. Hoboken, New Jersey: Wiley; 2008.
8. Tai YC, Laforest R. Instrumentation aspects of animal PET. *Annu Rev Biomed Eng*. 2005;7:255–285.
9. Carini DJ, Duncia JV, Aldrich PE, et al. Nonpeptide angiotensin II receptor antagonists: the discovery of a series of *N*-(biphenylmethyl)imidazoles as potent, orally active antihypertensives. *J Med Chem*. 1991;34:2525–2547.
10. Verjans JWH, Lovhaug D, Narula N, et al. Noninvasive imaging of angiotensin receptors after myocardial infarction. *JACC Cardiovasc Imaging*. 2008;1:354–362.
11. Arksey N, Hadizad T, Ismail B, et al. Synthesis and evaluation of the novel 2-[¹⁸F]fluoro-3-propoxy-triazole-pyridine-substituted losartan for imaging AT₁ receptors. *Bioorg Med Chem*. 2014;22:3931–3937.
12. Wong PC, Price WA, Chiu AT, et al. Nonpeptide angiotensin II receptor antagonists. XI. Pharmacology of EXP3174: an active metabolite of DuP 753, an orally active antihypertensive agent. *J Pharmacol Exp Ther*. 1990;255:211–217.
13. Fabiani ME, Dinh DT, Nassis L, Casley DJ, Johnston CI. In vivo inhibition of angiotensin receptors in the rat kidney by candesartan cilexetil: a comparison with losartan. *Am J Hypertens*. 2000;13:1005–1013.
14. Tan J, Wang H, Leenen FH. Increases in brain and cardiac AT₁ receptor and ACE densities after myocardial infarct in rats. *Am J Physiol Heart Circ Physiol*. 2004;286:H1665–H1671.
15. Almansa C, Gomez LA, Cavalcanti FL, et al. Diphenylpropionic acids as new AT₁ selective angiotensin II antagonists. *J Med Chem*. 1996;39:2197–2206.
16. Almansa C, Gomez LA, Cavalcanti FL, de Arriba AF, Garcia-Rafanell J, Forn J. Synthesis and structure-activity relationship of a new series of potent AT₁ selective angiotensin II receptor antagonists: 5-(biphenyl-4-ylmethyl)pyrazoles. *J Med Chem*. 1997;40:547–558.
17. Parasuraman S, Raveendran R. Measurement of invasive blood pressure in rats. *J Pharmacol Pharmacother*. 2012;3:172–177.
18. Lourenco CM, Houle S, Wilson AA, DaSilva JN. Characterization of (*R*)-[¹¹C]rolipram for PET imaging of phosphodiesterase-4: in vivo binding, metabolism, and dosimetry studies in rats. *Nucl Med Biol*. 2001;28:347–358.
19. Lortie M, DaSilva JN, Kirkpatrick SA, et al. Analysis of [¹¹C]methyl-candesartan kinetics in the rat kidney for the assessment of angiotensin II type 1 receptor density in vivo with PET. *Nucl Med Biol*. 2013;40:252–261.
20. International Commission on Radiological Protection (ICRP). Radiation dose to patients from radiopharmaceuticals. ICRP publication 53. *Ann ICRP*. 1987;18:1–377.
21. International Commission on Radiological Protection (ICRP). Radiation dose to patients from radiopharmaceuticals (addendum 2 to ICRP publication 53). ICRP Publication 80. *Ann ICRP*. 1998;28:1–126.
22. Kinahan PE, Fletcher JW. Positron emission tomography-computed tomography standardized uptake values in clinical practice and assessing response to therapy. *Semin Ultrasound CT MR*. 2010;31:496–505.
23. Thomas AJ, DaSilva JN, Lortie M, et al. PET of (*R*)-¹¹C-rolipram binding to phosphodiesterase-4 is reproducible and sensitive to increased norepinephrine in the rat heart. *J Nucl Med*. 2011;52:263–269.
24. Chang RS, Lotti VJ. Angiotensin receptor subtypes in rat, rabbit and monkey tissues: relative distribution and species dependency. *Life Sci*. 1991;49:1485–1490.
25. Michel MC, Foster C, Brunner HR, Liu L. A systematic comparison of the properties of clinically used angiotensin II type 1 receptor antagonists. *Pharmacol Rev*. 2013;65:809–848.
26. Dickstein K, Timmermans P, Segal R. Losartan: a selective angiotensin II type 1 (AT₁) receptor antagonist for the treatment of heart failure. *Expert Opin Investig Drugs*. 1998;7:1897–1914.
27. Diez J. Review of the molecular pharmacology of losartan and its possible relevance to stroke prevention in patients with hypertension. *Clin Ther*. 2006;28:832–848.
28. Prokop A, Davidson JM. Nanovehicular intracellular delivery systems. *J Pharm Sci*. 2008;97:3518–3590.
29. Mejia AA, Nakamura T, Masatoshi I, Hatazawa J, Masaki M, Watanuki S. Estimation of absorbed doses in humans due to intravenous administration of fluorine-18-fluorodeoxyglucose in PET studies. *J Nucl Med*. 1991;32:699–706.
30. Pauleit D, Floeth F, Herzog H, et al. Whole-body distribution and dosimetry of *O*-(2-[¹⁸F]fluoroethyl)-*L*-tyrosine. *Eur J Nucl Med Mol Imaging*. 2003;30:519–524.
31. Obrzut SL, Koren AO, Mandelkern MA, Brody AL, Hoh CK, London ED. Whole-body radiation dosimetry of 2-[¹⁸F]fluoro-A-85380 in human PET imaging studies. *Nucl Med Biol*. 2005;32:869–874.
32. Vanderheyden PM, Fierens FL, De Backer JP, Fraeyman N, Vauquelin G. Distinction between surmountable and insurmountable selective AT₁ receptor antagonists by use of CHO-K1 cells expressing human angiotensin II AT₁ receptors. *Br J Pharmacol*. 1999;126:1057–1065.
33. Christ DD. Human plasma protein binding of the angiotensin II receptor antagonist losartan potassium (DuP 753/MK 954) and its pharmacologically active metabolite EXP3174. *J Clin Pharmacol*. 1995;35:515–520.